

---

# MAXIMUM TRANSMISSION REACH FOR OPTICAL SIGNALS IN ELASTIC OPTICAL NETWORKS EMPLOYING BAND DIVISION MULTIPLEXING

---

**Esteban Paz**  
epaz@udec.cl  
Electrical Engineering Department  
Universidad de Concepcion

**Gabriel Saavedra**  
gasaavedra@udec.cl  
Electrical Engineering Department  
Universidad de Concepcion

## ABSTRACT

Multi-band transmission systems have emerged as a potential answer to the limited capacity of silica based optical fiber. It is based on utilizing the complete low-loss region of optical fibers. Additionally, elastic optical networks (EON) were proposed to efficiently manage limited resources in optical networks. The selection of route, modulation format and spectrum is the main problem that requires solving to operate an EON. Understanding how linear and nonlinear impairments accumulate during propagation in an optical fibre link is essential to solve this problem. Here we present a study on the maximum reach optical signals can propagate in a multi-band environment for a variety of modulation formats with commonly used threshold values in EON.

## 1 Introduction

Optical fibres underpin the global telecommunications infrastructure and carry over 95% of the data traffic in the world. However, it has been acknowledged that the capacity of optical fibres is not infinite, and that nonlinear effects that occur while information is propagated through optical fibres impose a limit on the maximum achievable information rates of optical communication systems [1, 2, 3, 4]. To sustain the ever-increasing demand for data new or alternative solutions for optical communication systems are needed. Due to the large and unused available spectrum of optical fibres, adopting multiple transmission windows (multi-band) to transmit information can lead to capacity increases for optical communication systems. In fact, projections for the next 20 years have highlighted the potential of this solution to overcome the so-called capacity crunch imposed by the nonlinear nature of silica based optical fibres [3]. Although adopting this solution conveys many technological challenges in terms of optical devices and integration [5, 6] it is the most promising solution to maintain the thousand of kilometres of optical fibre infrastructure installed around the world. Despite this, the use of multiple transmission bands for transmission of signal enhances the nonlinear interactions between signals, that depend on the power of the transmitted signal and bandwidths [7, 8, 9]. One of the main challenges to tackle in this multi-band transmission regime is the presence of inter-channel stimulated Raman scattering (ISRS) that transfers energy between the co-propagating channels and dominates the system performance [8, 10, 11, 12].

On the networking scenario, elastic optical networks (EONs) were proposed to overcome the limitations of WDM networks, using flexible resource allocation based on the demand of the users [13, 14, 15, 16, 17]. In order to do this, the optical spectrum is divided into frequency slots units (FSUs) of 12.5 or 6.25 GHz, that are grouped together to provide the required transmission resources for a given user. This can lead to spectral savings compared to conventional WDM networks. The main task a network operator must solve is to assign a path, a spectral region and a modulation format, known as the Routing, Modulation Level and Spectrum Assignment (RMLSA) problem [18, 19, 20, 21, 22, 23]. To select the modulation format the physical impairments accumulated during propagation need to be considered, as they limit the maximum reach a signal can travel and be detected complying with the quality of service required by the user or network operator.

Multi-band transmission, also known as band division multiplexing (BDM), can provide significant benefits to EONs operators, allowing them to support a larger number of users. However, in this scenario the RMLSA becomes a com-

plex problem, as the nonlinear interactions arising from inter-channel stimulated Raman scattering introduce further physical limitations in the channel, translated into distinct performance for each transmission band. In this work we study the effect that linear and nonlinear noise accumulation in BDM systems has on the transmission reach for optical signals managed by an EON operator. Using fiber propagation models [10, 24] we estimate the maximum transmission reach for a variety of modulation formats commonly used in EONs for each transmission band in a BDM network.

## 2 Methodology

To assign a wavelength and a modulation format for a user in EONs it is necessary to know the maximum transmission distance that an optical signal can travel to ensure a minimum quality of service for the user. The quality of service is typically ensured when the user exhibits a bit-error-rate (BER) lower than a predetermined threshold. Physical impairments, such as amplified spontaneous emission (ASE) noise, chromatic dispersion and nonlinear effects [25] degrade the received signal-to-noise ratio (SNR), and thus, increase the BER of a transmission. To achieve maximum transmission distance, the optical power launched into each fiber needs to be optimized to balance the effects of linear and nonlinear impairments, which have a strong dependence on the signal wavelength. To provide general conclusions, we compute a mean SNR for every transmission band considered in the system under study.

This section presents the methodology used to compute the per band SNR, and the parameters of the system under consideration.

### 2.1 Transmission system model

In this work the signal-to-noise ratio (SNR) was used as the performance metric to estimate the maximum transmission reach for each modulation format. The SNR was calculated as follows:

$$SNR_{ch} = \frac{P_{ch}}{P_{ASE,ch} + \eta_{P_{ch}} P_{ch}^3}, \quad (1)$$

where  $P_{ch}$  is the launch power of channel  $ch$ ,  $P_{ASE,ch}$  corresponds to the amplified spontaneous emission (ASE) noise power in the channel bandwidth, and  $\eta_{ch}$  is the nonlinear interference (NLI) coefficient of said channel. The latter term ( $\eta_{P_{ch}} P_{ch}^3$ ) in the denominator corresponds to the nonlinear "noise" generated during transmission, and it depends on the signal power and wavelength.

Here we consider a system amplified by lumped optical amplifiers (such as EDFA, PDFA, NDFA and TDFS [5, 6]), then, the ASE noise contribution in Eq. 1 is given by:

$$P_{ASE,ch} = 2n_{sp}hv(G - 1), \quad (2)$$

where  $n_{sp}$  is the population inversion factor,  $h$  is Planck's constant,  $v$  the frequency of the channel of interest and  $G = \alpha L$  is the amplifier gain, being  $\alpha$  the attenuation coefficient of the fiber and  $L$  the span length. Both the channel frequency and the amplifier gain vary significantly withing the bandwidth of interest, and thus, the ASE noise is expected to vary in the same manner.

The calculation of the nonlinear coefficients  $\eta_{ch}$  was performed utilizing a closed-form approximation of the Gaussian noise model from [24]. The nonlinear interference (NLI) coefficient  $\eta$  is dominated by modified signal power profile from inter-channel stimulated Raman scattering (ISRS), single and cross phase modulations (SPM and XPM respectively), and Four wave mixing (FWM). The NLI coefficient was obtained using:

$$\eta(f_i)_{ch,P} \approx \sum_{j=1}^n \left[ \frac{P_{i,j}}{P_i} \right]^2 \cdot [\eta_{SPM,j}(f_i) + \eta_{XPM,j}(f_i)] \quad (3)$$

where  $P_{i,j}$  is the power of channel  $i$  launched into the  $j$ -th span. The contribution of SPM ( $\eta_{SPM,j}$ ) is given by:

$$\eta(f_i)_{SPM} \approx \frac{4}{9} \frac{\gamma^2}{B_i^2} \frac{\pi}{\phi_i \bar{\alpha} (2\alpha + \bar{\alpha})} \cdot \left[ \frac{T_i - \alpha^2}{a} \operatorname{arcsinh}\left(\frac{\phi - iB_i^2}{a\pi}\right) + \frac{A^2 - T_i}{A} \operatorname{arcsinh}\left(\frac{\phi - iB_i^2}{A\pi}\right) \right], \quad (4)$$

with  $\phi_i = \frac{2}{3}\pi^2(\beta_2 + 2\pi\beta_3 f_i)$ ,  $A = \alpha + \bar{\alpha}$ ,  $T_i = (\alpha + \bar{\alpha} - P_{tot} C_r f_i)^2$ .

$B_i$  is the channel  $i$  bandwidth,  $\bar{\alpha}$  is considered equal to  $\alpha$ ,  $C_r$  is the Raman gain spectrum slope,  $P_{tot}$  is the total launch power,  $\beta_2$  is the group velocity dispersion and  $\beta_3$  is the third-order dispersion parameter.

The XPM ( $\eta_{XPM,j}$ ) contribution is given by:

$$\eta(f_i)_{XPM} \approx \frac{32}{27} \sum_{k=1, k \neq i}^{N_{ch}} \left(\frac{P_k}{P_i}\right)^2 \frac{\gamma^2}{B_k \phi_{i,k} \bar{\alpha} (2\alpha + \bar{\alpha})} \cdot \left[ \frac{T_k - \alpha^2}{\alpha} \arctan\left(\frac{\phi - i, kB_i^2}{\alpha}\right) + \frac{A^2 - T_k}{A} \arctan\left(\frac{\phi - i B_i^2}{A}\right) \right], \quad (5)$$

with  $\phi_{i,k} = 2\pi^2(f_k - f_i)[\beta_2 + \pi\beta_3(f_k + f_i)]$ , as is shown in [1].

Further, to relate the received SNR to a maximum transmission reach, BER thresholds conventionally used in coherent transmission systems and EONs were used. The relationship between SNR and BER, assuming an additive white Gaussian noise channel, is given by [26]:

$$BER_{\Lambda-PSK} = \frac{1}{2} \operatorname{erfc} \left( \sqrt{\frac{SNR \Delta_{ref}}{\lambda \frac{B_{ch}}{B_{ch}}}} \right), \quad (6)$$

$$BER_{\Lambda-QAM} = \frac{1}{\lambda} \left( 1 - \frac{1}{\sqrt{\Lambda}} \right) \cdot \operatorname{erfc} \left( \sqrt{\frac{3 SNR \Delta_{ref}}{2(\Lambda - 1) \frac{B_{ch}}{B_{ch}}}} \right), \quad (7)$$

where  $\Lambda$  is the constellation of cardinality,  $\lambda$  represents the bits encoded in each constellation symbol, such that  $\Lambda = 2^\lambda$ .  $\Delta_{ref}$  and  $B_{ch}$  represent the reference and channel bandwidth.

## 2.2 System Parameters

Here we consider that the transmission link is based on standard single mode fiber (SMF) and the coherent system employs BDM. A total of 2720 FSUs were occupied centered in the S band, yielding a total bandwidth of 34THz, from 1365-1615 nm. The bandwidth was selected to cover the E, S, C and L bands. The O band was not considered due to the enhancement of nonlinear interactions as the zero dispersion wavelengths is approached, and the reduced accuracy of the GN model in that region. The Raman gain coefficient ( $C_r$ ) was approximated assuming a linear increase for frequency shifts between 0-13 THz, for larger frequency shifts the value was assumed to be 0. Further, we assume that the signal launch power is the same in every transmission band.

The simulation parameters are shown in table 1.

Parameter	Symbol	Value
<i>Fiber parameters</i>		
Attenuation Coefficient @ 1550 nm (C band mean)	$\alpha$	0.165dB/km
Attenuation Coefficient @ 1590 nm (L band mean)	$\alpha$	0.171dB/km
Attenuation Coefficient @ 1495 nm (S band mean)	$\alpha$	0.177dB/km
Attenuation Coefficient @ 1410 nm (E band mean)	$\alpha$	0.217dB/km
Dispersion Coefficient	$D$	21.3 ps/nm/km
Dispersion Slope	$S$	0.067 ps/nm <sup>2</sup> /km
Raman gain coefficient @ 13 THz	$C_r$	0.028 (1/W/km)
Nonlinear coefficient	$\gamma$	1.2 W <sup>-1</sup> km <sup>-1</sup>
Optical Reference Bandwidth	$\Delta_{ref}$	12.5GHz
Span length	$L$	100km
<i>Amplifier parameters</i>		
Noise figure	$F$	5dB
<i>Signal parameters</i>		
Central frequency WDM	$\nu$	1480nm(200.67THz)
Symbol Rate	$R$	12.5GBaud
Channel spacing	$\Delta f$	12.5GHz
Optical bandwidth	BW	2720FSUs(34THz)

Table 1: Fiber parameters for maximum reach calculation

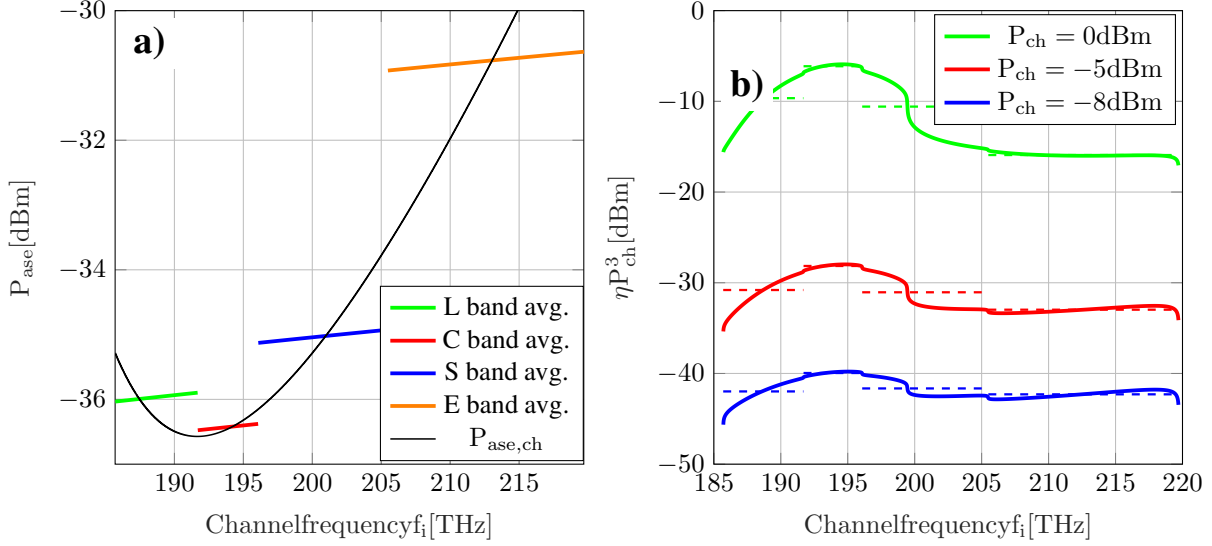


Figure 1: **a)** ASE noise power as a function of channel frequency. Solid black line represents ASE noise for every channel under study, colored lines show the average ASE in every transmission band. **b)** Nonlinear Interference noise  $\eta P_{ase}^3$  as a function of the channels frequency, for  $P_{launch} = -8$  dBm,  $-5$  dBm,  $0$  dBm.

### 3 Results

First we study the noise generation over the entire bandwidth of interest in a single fiber span. To do so, Eq. (2) and Eq. (3) were used to calculate the ASE and NLI coefficient, respectively. The ASE noise power arising from optical amplification ( $P_{ase,ch}$ ) as a function of the channel frequency is presented in Fig. 1 a). The  $P_{ase,ch}$  for each channel within the studied bandwidth is shown in solid black. Additionally, it is observed that  $P_{ase,ch}$  is segmented in four linear sections. These partitions are the result of taking the average attenuation coefficient for each band, resulting on an average gain and thus a linear noise power according to equation (2). The  $P_{ase}$  corresponding to the E band is  $6$  dB higher than the noise power of the C band. This agrees with theory, since the frequencies in the E band present a higher attenuation coefficient, and consequently a higher gain is needed for compensation. In this work the average  $P_{ase}$  per band was used for the calculations of maximum reach, assuming an average loss in each band.

Secondly, the NLI coefficient for each band was obtained for the system under study. The values of  $\eta$  from Eq. (3) were computed as a function of the channels frequency at a variety of launch powers, from  $-25$  to  $10$  dBm. In Figure 1 b) particular plots for  $P_{launch} = -8$  dBm,  $-5$  dBm,  $0$  dBm of NLI noise, corresponding to the second term in the denominator of Eq. (1), are presented. An increase in NLI noise is observed for the lower frequencies of the spectrum, corresponding to the region where the channels experience amplification due to the power transfer arising from ISRS. Additionally, it can be observed that a lower launch power translates into a lower value of NLI noise. For simplicity, the NLI noise in each band was averaged, shown with dashed lines in Fig. 1 b).

The SNR after one fiber span was calculated as a function of the signal launch power using Eq. (1). The results are shown in Fig. 2 a) from which is observable that the L band takes a maximum  $27.1$  dB SNR at  $-7.5$  dBm, followed by the C band with SNR= $26.8$  dB at  $-8$  dBm. The lowest maximum SNR occurs on the E band with a value of  $23.8$  dB at  $-5.5$  dBm.

From Figure 1 b) one can observe that the lowest average NLI noise value at  $P_{launch} = -8$  dBm happens around  $185 - 190$  THz and  $205 - 215$  THz, corresponding to the L band and part of the C and S bands respectively. Remark that the lowest ASE noise power in Figure 1 a) is found in the L and S bands, so the resulting SNRs in L and C bands are expected. The resulting SNR values are resumed in Table 2. Which indicate the maximum SNR obtained paired with its optimal launch power for each band.

Now, Fig. 2 b) presents the maximum SNR for each transmission band as a function of the number of spans. This was obtained assuming incoherent addition of NLI as follows:

$$SNR_{ch} = \frac{P_{ch}}{NP_{ASE,ch} + N\eta P_{ch}^3}, \quad (8)$$

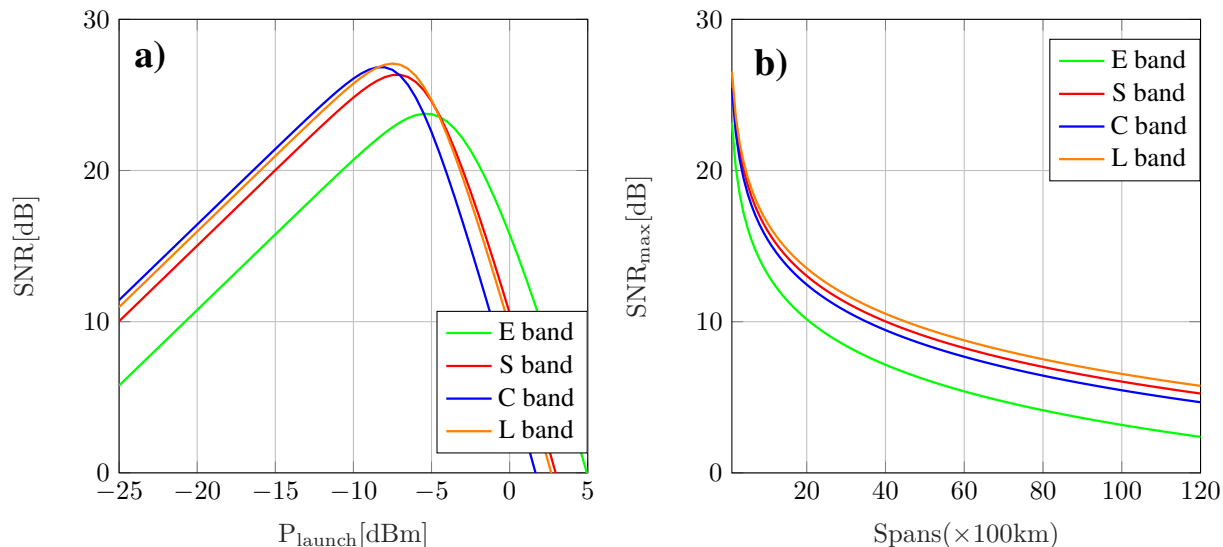


Figure 2: **a)**SNR as a function of the Launch Power  $P_{\text{launch}}$  in dBm. **b)**SNR in function of the number of spans

Band	SNR[dB]	$P_{\text{launch}}$ [dBm]
E (1365nm - 1460nm)	23.75	-5.5
S (1460nm - 1530nm)	26.33	-7
C (1530nm - 1565nm)	26.82	-8
L (1565nm - 1615nm)	27.07	-7.5

Table 2: Maximum SNR per band and its respective launch power

where  $N$  is the number of transmission spans.

In these calculations a signal launch power of  $P_{\text{launch}} = -7\text{dBm}$  was considered for every band, and consequently the starting SNR for each band might be slightly lower than the optimum SNR. Considering that the L band has the higher SNR among the studied bands at  $-7\text{dBm}$ , therefore, it shows the highest SNR throughout all the spans, since a proportional decay is observed for every transmission band. In the same manner, the E band presents the lowest SNR as a function of the number of spans.

The results presented so far show the generation and accumulation of noise for a optical signal propagating in a multi band transmission system. A network operator uses this information to estimate the maximum a distance can be transmitted and detected with a given quality of service. Here we provide the bit rates achieved by signal in a single FSU over 2 polarizations with and without FEC overhead for a variety of modulation formats of interest. Then we obtain the maximum transmission reach for said signals. The modulation formats considered here are: BPSK, QPSK, 16QAM, 64QAM and 256QAM; the BER thresholds ( $\text{BER}_{\text{th}}$ ) considered are:  $4.7 \times 10^{-3}$  [27],  $10^{-6}$ ,  $10^{-9}$  [28, 29, 30]. The bit rates achieved in a single FSU are shown in Table 3.

Modulation format	$\text{BER}_{\text{th}} = 4.7 \times 10^{-3}$	$\text{BER}_{\text{th}} = 10^{-6} \& 10^{-9}$
	Net bit rate [Gb/s]	Net bit rate [Gb/s]
BPSK	23	25
QPSK	46	50
16QAM	92	100
64QAM	140	150
256QAM	186	200

Table 3: Net bit rate for each modulation formation format using a single FSU

The relationship between the SNR and BER is shown in Fig. 3, results obtained using Eqs. (7) and (6).

For BPSK, which is the less complex modulation format present, one can notice that a lower SNR is required in comparison to more complex formats for a fixed BER value. In general, as the modulation formats is able to transmit

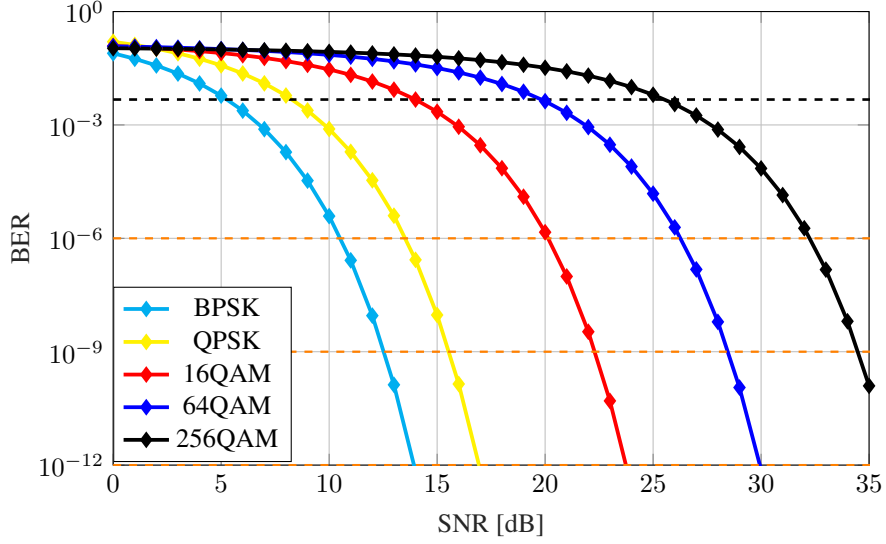


Figure 3: Relationship between SNR and BER for different M-PSK and M-QAM modulation formats

more bits in each symbol a higher SNR is required to obtain a fixed BER. Additionally, the studied BER thresholds are shown with dashed horizontal lines.

The maximum reach the modulation formats studied can achieve for the BER thresholds under consideration are summarized in Tables 4, 5, 6. These values together with the ones presented in Table 3 can be used by an EON operator as the input to solve the RMLSA problem.

Modulation format	BPSK	QPSK	16QAM	64QAM	256QAM
SNR threshold	5.3 dB	8.3 dB	14 dB	19.8 dB	25.5 dB
Band	Reach[spans]	Reach[spans]	Reach[spans]	Reach[spans]	Reach [spans]
E	61	30	8	2	0
S	118	59	16	4	1
C	103	52	14	3	1
L	133	66	18	4	1

Table 4: Maximum reach for a BER threshold of  $4.7 \times 10^{-3}$

Modulation format	BPSK	QPSK	16QAM	64QAM	256QAM
SNR threshold	10.5 dB	13.5 dB	20.2 dB	26.3 dB	32.3 dB
Band	Reach[spans]	Reach[spans]	Reach[spans]	Reach[spans]	Reach [spans]
E	18	9	1	0	0
S	35	18	3	0	0
C	31	15	3	0	0
L	40	20	4	1	0

Table 5: Maximum reach for a BER threshold of  $10^{-6}$

Modulation format	BPSK	QPSK	16QAM	64QAM	256QAM
SNR threshold	12.5 dB	15.6 dB	22.3 dB	28.5 dB	34.6 dB
Band	Reach[spans]	Reach[spans]	Reach[spans]	Reach[spans]	Reach [spans]
E	11	5	1	0	0
S	22	11	2	0	0
C	19	9	2	0	0
L	25	12	2	0	0

Table 6: Maximum reach for a BER threshold of  $10^{-9}$

## Conclusion

In this work we computed the maximum reach for a variety of modulation formats with commonly used threshold values in EONs. This was achieved by computing the particular SNR for the E,S,C and L bands using a closed form approximation of the Gaussian noise model in presence of ISRS, which allowed us to obtain the nonlinear coefficients needed for the SNR calculation.

## Acknowledgements

The authors thank A. Lozada (USM) for helpful feedback and discussions.

## References

- [1] P. P. Mitra and J. B. Stark, "Nonlinear limits to the information capacity of optical fibre communications." *Nature*, vol. 411, no. 6841, pp. 1027–1030, 2001.
- [2] R. J. Essiambre, G. Kramer, P. J. Winzer, G. J. Foschini, and B. Goebel, "Capacity Limits of Optical Fiber Networks," *Journal of Lightwave Technology*, vol. 28, no. 4, pp. 662–701, Feb 2010.
- [3] P. J. Winzer, D. T. Neilson, and A. R. Chraplyvy, "Fiber-optic transmission and networking: the previous 20 and the next 20 years," *Optics express*, vol. 26, no. 18, pp. 24 190–24 239, 2018.
- [4] A. D. Ellis, N. Mac Suibhne, D. Saad, and D. N. Payne, "Communication networks beyond the capacity crunch," *Philosophical Transactions of the Royal Society A: Mathematical, Physical and Engineering Sciences*, vol. 374, no. 2062, 2016.
- [5] A. Napoli, N. Costa, J. K. Fischer, J. ao Pedro, S. Abrate, N. Calabretta, W. Forysiak, E. Pincemin, J. P.-P. Gimenez, C. Matrakidis, G. Roelkens, and V. Curri, "Towards multiband optical systems," in *Advanced Photonics 2018 (BGPP, IPR, NP, NOMA, Sensors, Networks, SPPCom, SOF)*. Optical Society of America, 2018, p. NeTu3E.1. [Online]. Available: <http://www.osapublishing.org/abstract.cfm?URI=Networks-2018-NeTu3E.1>
- [6] A. Napoli, N. Calabretta, J. K. Fischer, N. Costa, S. Abrate, J. Pedro, V. Lopez, V. Curri, D. Zibar, E. Pincemin *et al.*, "Perspectives of multi-band optical communication systems," in *2018 23rd Opto-Electronics and Communications Conference (OECC)*. IEEE, 2018, pp. 1–2.
- [7] P. Bayvel, R. Maher, T. Xu, G. Liga, N. A. Shevchenko, D. Lavery, A. Alvarado, and R. I. Killey, "Maximizing the optical network capacity," *Philosophical Transactions of the Royal Society A: Mathematical, Physical and Engineering Sciences*, vol. 374, no. 2062, p. 20140440, 2016.
- [8] D. Semrau, R. Killey, and P. Bayvel, "Achievable rate degradation of ultra-wideband coherent fiber communication systems due to stimulated raman scattering," *Optics express*, vol. 25, no. 12, pp. 13 024–13 034, 2017.
- [9] G. Saavedra, M. Tan, D. J. Elson, L. Galdino, D. Semrau, M. A. Iqbal, I. D. Phillips, P. Harper, A. Ellis, B. C. Thomsen, D. Lavery, R. I. Killey, and P. Bayvel, "Experimental analysis of nonlinear impairments in fibre optic transmission systems up to 7.3 thz," *Journal of Lightwave Technology*, vol. 35, no. 21, pp. 4809–4816, Nov 2017.
- [10] D. Semrau, R. I. Killey, and P. Bayvel, "The gaussian noise model in the presence of inter-channel stimulated raman scattering," *Journal of Lightwave Technology*, vol. 36, no. 14, pp. 3046–3055, 2018.
- [11] M. Cantono, D. Piloni, A. Ferrari, and V. Curri, "Introducing the generalized gn-model for nonlinear interference generation including space/frequency variations of loss/gain," *arXiv preprint arXiv:1710.02225*, 2017.
- [12] M. Cantono, J. L. Auge, and V. Curri, "Modelling the impact of srs on nli generation in commercial equipment: an experimental investigation," in *Optical Fiber Communication Conference*. Optical Society of America, 2018, pp. M1D–2.
- [13] O. Gerstel, M. Jinno, A. Lord, and S. J. B. Yoo, "Elastic optical networking: a new dawn for the optical layer?" *IEEE Communications Magazine*, vol. 50, no. 2, pp. s12–s20, 2012.
- [14] P. Layec, A. Morea, F. Vacondio, O. Rival, and J. Antona, "Elastic optical networks: The global evolution to software configurable optical networks," *Bell Labs Technical Journal*, vol. 18, no. 3, pp. 133–151, 2013.
- [15] N. Sambo, P. Castoldi, F. Cugini, G. Bottari, and P. Iovanna, "Toward high-rate and flexible optical networks," *IEEE Communications Magazine*, vol. 50, no. 5, pp. 66–72, 2012.
- [16] V. López, L. Velasco *et al.*, "Elastic optical networks," *Architectures, Technologies, and Control, Switzerland: Springer Int. Publishing*, 2016.

- [17] S. Talebi, F. Alam, I. Katib, M. Khamis, R. Salama, and G. N. Rouskas, "Spectrum management techniques for elastic optical networks: A survey," *Optical Switching and Networking*, vol. 13, pp. 34–48, 2014.
- [18] J. Yuan, R. Zhu, Y. Zhao, Q. Zhang, X. Li, D. Zhang, and A. Samuel, "A Spectrum Assignment Algorithm in Elastic Optical Network with Minimum Sum of Weighted Resource Reductions in all Associated Paths," *Journal of Lightwave Technology*, 2019.
- [19] A. Fontinele, I. Santos, J. N. Neto, D. R. Campelo, and A. Soares, "An Efficient IA-RMLSA Algorithm for Transparent Elastic Optical Networks," *Computer Networks*, 2017.
- [20] T. Hashimoto, K. I. Baba, and S. Simojo, "A study on routing, modulation level, and spectrum allocation algorithms for elastic optical path networks," in *ICP 2012 - 3rd International Conference on Photonics 2012, Proceedings*, 2012.
- [21] X. Luo, Y. Zhao, X. Chen, L. Wang, M. Zhang, J. Zhang, Y. Ji, H. Wang, and T. Wang, "Manycast routing, modulation level and spectrum assignment over elastic optical networks," *Optical Fiber Technology*, 2017.
- [22] M. Klinkowski, K. Walkowiak, and M. Jaworski, "Off-line algorithms for routing, modulation level, and spectrum assignment in elastic optical networks," in *2011 13th International Conference on Transparent Optical Networks*, June 2011, pp. 1–6.
- [23] K. Christodouloupoulos, I. Tomkos, and E. a. Varvarigos, "Elastic Bandwidth Allocation in Flexible OFDM-based Optical Networks," *Journal of Lightwave Technology*, vol. 29, no. 9, pp. 1354 – 1366, 2011. [Online]. Available: [http://ieeexplore.ieee.org/xpls/abs/\\_all.jsp?arnumber=5727897&tag=1](http://ieeexplore.ieee.org/xpls/abs/_all.jsp?arnumber=5727897&tag=1)
- [24] D. Semrau, R. I. Killey, and P. Bayvel, "A closed-form approximation of the gaussian noise model in the presence of inter-channel stimulated raman scattering," *Journal of Lightwave Technology*, vol. 37, no. 9, pp. 1924–1936, 2019.
- [25] C. Politi, C. Matrakidis, and A. Stavdas, *A Tutorial on Physical-Layer Impairments in Optical Networks*. Springer US, 2013, pp. 5–29.
- [26] M. Salehi and J. Proakis, *Digital communications*. McGraw-Hill Education, 2007, vol. 31.
- [27] L. M. Zhang and F. R. Kschischang, "Staircase codes with 6% to 33% overhead," *Journal of Lightwave Technology*, vol. 32, no. 10, p. 1999–2002, 2014.
- [28] A. Fallahpour, H. Beyranvand, S. A. Nezamalhosseini, and J. A. Salehi, "Energy efficient routing and spectrum assignment with regenerator placement in elastic optical networks," *Journal of Lightwave Technology*, vol. 32, no. 10, pp. 2019–2027, 2014.
- [29] H. Beyranvand and J. A. Salehi, "A quality-of-transmission aware dynamic routing and spectrum assignment scheme for future elastic optical networks," *Journal of Lightwave Technology*, vol. 31, no. 18, pp. 3043–3054, 2013.
- [30] M. Aibin and K. Walkowiak, "Adaptive modulation and regenerator-aware dynamic routing algorithm in elastic optical networks," in *IEEE International Conference on Communications (ICC)*. London, UK: IEEE, 2015, pp. 5138–5143.